10^{th} International Conference on Fracture Mechanics of Concrete and Concrete Structures
FraMCoS-X
G. Pijaudier-Cabot, P. Grassl and C. La Borderie (Eds)

RETROFITTING UNREINFORCED MASONRY BUILDINGS WITH A STRAIN-HARDENING CEMENT-BASED COMPOSITE TO ENHANCE SEISMIC RESISTANCE

MARISKA KOTZE*, GERT C. VAN ROOYEN† GIDEON P.A.G. VAN ZIJL‡

*University of Stellenbosch
Stellenbosch, South Africa
e-mail: 18179142@sun.ac.za

†University of Stellenbosch
Stellenbosch, South Africa
e-mail: gcvr@sun.ac.za

‡University of Stellenbosch
Stellenbosch, South Africa
e-mail: gvanzijl@sun.ac.za

Key words: SHCC, Masonry, Seismic

Abstract. In South Africa there are many low-rise, unreinforced, load-bearing masonry (ULM) buildings in seismic zones due to shortcomings in South Africa′s design codes. These buildings pose a great risk to their occupants in the case of seismic activity . A possible solution is to retrofit these buildings with a strain-hardening cement-based composite (SHCC) overlay. It is postulated that the strain hardening characteristic of the SHCC overlay may sufficiently increase the ductility of such buildings to prevent collapse during seismic activity. This paper discusses the effects SHCC have on the damaged behaviour of masonry walls under in-plane seismic action. These effects were evaluated using experimental pushover tests with different retrofitting techniques. From the tests, it was concluded that adding an SHCC overlay increased the in-plane shear resistance of a masonry wall. The ductility was improved by introducing debonding strips between the masonry wall and SHCC overlay. The SHCC retrofitting scheme was numerically optimised using non-linear finite element (FE) analyses. Masonry was modelled using a smeared crack model with a Rankine-Hill material to allow for tensile softening and compression hardening followed by softening as well as an Engineering-Masonry model to allow for multi-directional loading. The interface between the masonry wall and SHCC overlay was modelled using a Coulomb friction model. The SHCC overlay was modelled using a Rankine-Rankine model with compression and tension hardening.

1 INTRODUCTION

There were no seismic design specifications in the South African design codes before 1989, therefore there are many ULM buildings that were constructed in seismic areas [1].These buildings need to be retrofitted in order to withstand seismic events should they occur.

SHCC was proposed by [2] as a possible bonded overlay retrofitting solution to increase the ductility and shear resistance of ULM buildings to better resist seismic action. De Beer [2] developed a sprayable SHCC mix to apply on masonry walls. He conducted extensive experimental research, consisting of small

masonry triplets tests with and without SHCC overlay and larger shear dominant beam specimens, also with and without SHCC overlay. The aim of these tests were to obtain the model parameters, namely the compression strength of mortar and individual bricks, shear strength of brick-mortar bond, SHCC-brick shear bond strength, SHCC overlay shear strength, tensile strength and Young's modulus.

The ductility factor (μ), as seen in Equation 1 was used to determine if the SHCC overlay improved the overall ductility of the masonry.

$$\mu = \frac{\delta_u}{\delta_y} \tag{1}$$

δ_u is defined as the in-plane shearing deformation when the post peak shearing resistance has reduced by 80%, and δ_y is the yield shearing deformation at the intersection of the elasic-plastic bilinear approximation of the load deformation response as defined by Mahmood and Ingham [3]. The ductility factor of the beam specimens, with and without SHCC overlay, tested by De Beer [2] were on average 1.8 with a CoV of 0.187. It was therefore concluded by that although the SHCC increased the shear resistance of the beam specimens, the ductility remained unaffected, and further research had to be conducted on how to improve the ductility of the SHCC overlay.

Research conducted by De Jager [4] consisted of setting up FE models for the SHCC retrofitted masonry walls to further test and develop debonding strips as a way to increase the ductility of the SHCC overlay. Promising results were obtained that are discussed in detail in section 5. An energy contribution factor (ECF), as seen in in Equation 2, was developed to numerically illustrate the improved energy dissipation of the SHCC overlay with debonding strips in comparison to a fully bonded overlay.

$$ECF = \frac{\delta_{su} - \delta_{sy}}{\delta_{ru} - \delta_{ry}} \tag{2}$$

δ_s referes to the wall with debonding strips, and δ_r refers to the wall without debonding srips. The subscript y refers to the shearing displacement at a preselected shear force in the elastic region, and the subscript u refers to the displacement at the same force in the plastic region.

The experimental push-over tests conducted by [2] and [4] consisted of a 1150x935mm masonry wall, as illustrated in Figure 1, that was either single- (110 mm) or double-leaf (220 mm). The size of the test wall was selected to facilitate shear failure, as this is the failure that typically occurs during seismic events. It is also the typical size of the wall between openings in a building. It was supported at the top and bottom with a 100x400 mm concrete beam with 175 mm overhang on either side. A 345x345x89 H steel beam was placed om top of the concrete beam and the loads of the upper stories were applied to the steel beam through three rows of steel rods, two on each side, each with a cross-sectional area of $380mm^2$. The displacement was directly applied to the middle of the steel beam. The shear resistance of the wall was determined by displacing the steel beam a total of 20mm at a rate of 2mm/min and measuring the reaction force at the point of displacement. The boundary conditions were fixed at the bottom, and out of plane displacements were constrained. The top of the wall was fixed to the concrete beam by using strong mortar.

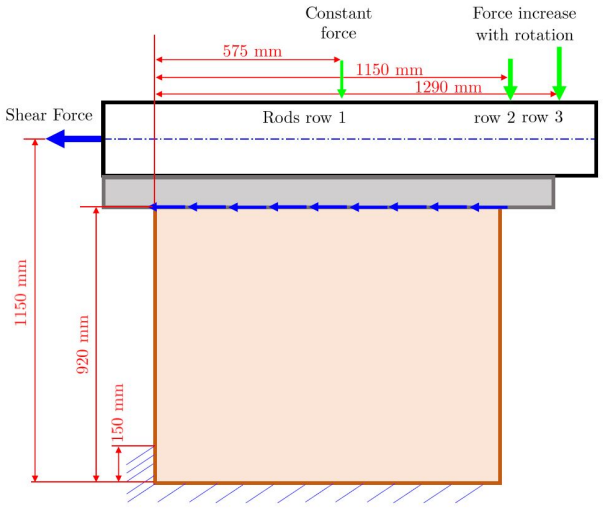

Figure 1: Basic setup of full scale shear wall test [2]

2 REPRESENTATIVE BUILDING

The aim of this study is to ultimately model a typical full scale building, as seen in Figure 2, with and without SHCC overlay.

Figure 2: Typical low income residential building in Cape Town/Stellenbosch

A simplified modal analysis will be done to determine the displacement of the building due to an earthquake, using a quasi-static approach. The bare building will be compared to the retrofitted building to determine the optimum configuration of the SHCC overlay.

3 NUMERICAL MODEL METHODOLOGY

All the elements shown in Figure 1 were modelled as 3D membranes except the steel rods that were modelled as 3D line trusses.

The finite element model was solved using a non-linear phased analysis. Firstly the own weight was applied to the model, followed by the pressure in the rods representing the weight of the upper stories, and lastly the incremental displacement was applied to the middle of the steel beam, in 0.2 mm increments. The force of the middle rod pair in the experimental setup, done by De Beer [2], was kept constant by means of springs, while the forces in the rods at the end increased as the horizontal displacement increased. Typical forces in the rods are illustrated in Figure 3 over time, as the displacement was applied in 2mm/min increments. These forces were measured by De Beer [2] in his experimental tests.

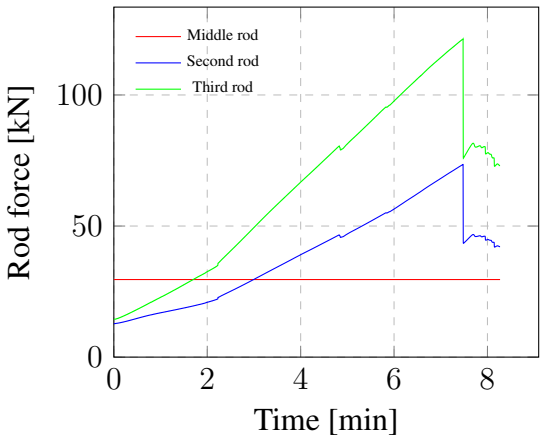

Figure 3: Rod forces

Masonry can be modelled either at macro level, that simulates the global behaviour of the structure, or meso level, where the behaviour of the masonry structure is simulated in more detail, however this is a computationally intensive approach. The macro level approach was chosen as the aim is to obtain a global representation of the model. The 15 mm SHCC overlay was modelled using a rotating smeared cracking model, with parameters as illustrated in Table 1. With the high tensile fracture energy, the pseudo-plastic post-cracking tensile behaviour of SHCC is simulated.

Table 1: Rotating smeared crack material model parameters for SHCC

Symbol	Value	Description
E	$15000 N/mm^2$	Young's modulus
ν	0.2	Poisson's ratio
ρ	2100 kg/m^3	Mass density
f_t	2.0 N/mm^2	Tensile strength
G_{ft}	10 N/mm	Fracture energy

To model masonry in Diana 10.2 there are two different material models namely, Engineering Masonry and Rankine-Hill. The Engineering Masonry material model is a smeared failure model that can simulate cyclic loading of masonry structures. The Rankine-Hill material

model is an anisotropic, multi-surface plasticity model that allows for tensile softening and compression hardening followed by softening. It should be noted that unloading in the Rankine-Hill model is elastic, and does not take crack closure into account in unloading [5]. Both these material models were used and compared. The parameters for the Rankine-Hill and Engineering Masonry material models are listed in Table 2 and 3 respectively. It should be noted that the values were obtained by starting with experimental values and adjusting them until a reasonably good correlation between the numerical model and the experimental tests were obtained. A double-leaf wall (220 mm) was used in this study, as the main focus is on load bearing masonry walls which are typically 220 mm wide.

Table 2: Rankine-Hill model parameters for masonry

Symbol	Value	Description
E	$1800N/mm^2$	Young's modulus
ν	0.22	Poisson's ratio
ρ	2100 kg/m^3	Mass density
ft_x	0.35 N/mm^2	Tensile strength (x)
ft_y	0.22 N/mm^2	Tensile strength (y)
fc_{ux}	20 N/mm^2	Compression strength (x)
fc_{uy}	20 N/mm^2	Compression strength (y)
Gt_x	0.15 N/mm	Fracture energy in tension (x)
Gt_y	0.1 N/mm	Fracture energy in tension (y)
Gc_x	2 N/mm	Fracture energy in compression (x)
Gc_y	2 N/mm	Fracture energy in compression (y)
ϵ_u	0.001	Ultimate compressive strain

The interface between the masonry wall and SHCC overlay was modelled using a Coulomb friction model, with cohesive strength of c = 2.3 MPa and friction angle of ϕ = 1.08 rad. These parameters were determined by De Beer [2] from the standard triplet test. The debonding strips discussed in section 5 were modelled as a weak interface between the SHCC overlay and the masonry. The steel beam and the concrete beam were modelled as linear elastic material.

Table 3: Engineering Masonry model parameters for masonry

Symbol	Value	Description
E_x	$1440N/mm^2$	Young's modulus (x)
E_y	$850N/mm^2$	Young's modulus (y)
G_{xy}	$350N/mm^2$	Shear modulus
ν	0.22	Poisson's ratio
ρ	2100 kg/m^3	Mass density
ft_y	0.15 N/mm^2	Tensile strength (y)
ft_r	0 N/mm^2	Residual tensile strength
fc	15 N/mm^2	Compression strength
Gt	0.1 N/mm	Fracture energy in tension
Gc	0.4 N/mm	Fracture energy in compression
Gs	0.5 N/mm	Fracture energy in shear
α	$0.8rad$	Diagonal crack angle
c	2.3 N/mm^2	Cohesion

3.1 Mesh

To determine the appropriate element type and mesh size, a mesh dependency analysis was done. Quadratic quadrilateral and quadratic triangular elements were considered with normal and high numerical integration respectively. The mesh dependencies are illustrated in Figure 4 and Figure 5. The figures illustrate shear force against mesh size, with the shear force taken at different displacement points.

It was found that quadrilateral elements with a 2x2 integration scheme does not follow any

significant trend, and therefore it does not deliver reliable results. Using a 3x3 integration scheme yields consistent results up to 9.5mm displacement for mesh sizes smaller than 30mm, as shown in Figure 4. Displacements larger than 9.5mm are however still mesh dependent and unreliable.

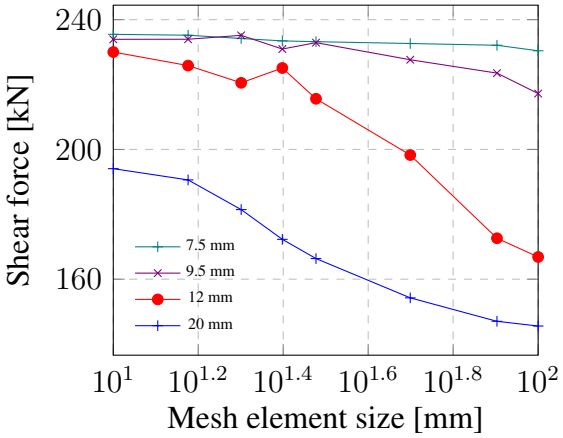

Figure 4: Quadrilateral element with 3x3 integration

The mesh dependency for quadratic triangular elements was done only with high integration. There is no difference between reduced, normal and high integration for quadratic triangular elements in Diana 10.2, as all these integration schemes use 3 integration points [6]. As shown in Figure 5, fairly consistent results were obtained for all displacements if the element size is 25 mm or less.

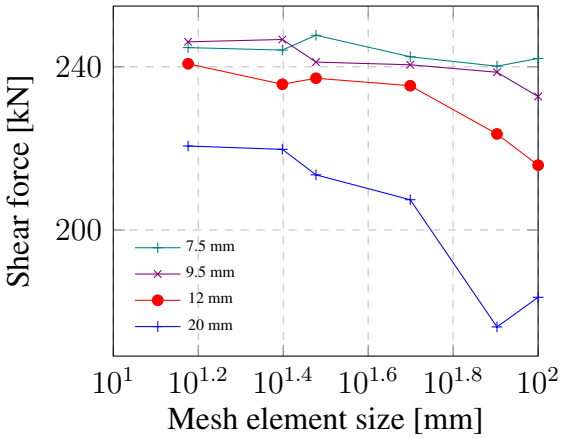

Figure 5: Triangular element with high integration

Consequently, a triangular mesh size of 25mm with higher order integration was selected for the models, as illustrated in Figure 6. The element is a six-node isoparametric triangular three dimensional plane stress element, referred to as a CT18GM element in Diana. The triangular mesh was also preferred above the quadrilateral due to the orientation of the mesh elements having an effect on where shear failure occurs. It was found by van Zijl et. al [7] that element sides are preferred directions for computational localization, therefore the triangular mesh will provide a better representation of the diagonal shear. The crack band width is defined as the square root of the finite element area to ensure objective fracture energy dissipation in crack formation through a single line of finite elements.

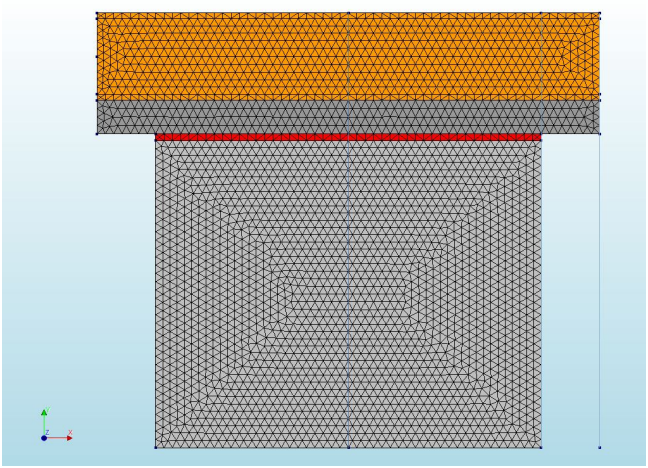

Figure 6: 25mm Triangular mesh of the shear wall model

4 EXPERIMENTAL AND NUMERICAL RESULTS

Figure 7 illustrates the shear force against displacement of two walls tested by De Beer [2] in comparison to the shear forces obtained from the non-linear finite element models, using both Rankine-Hill and Engineering-Masonry material models for the masonry. It can be seen that both the numerical models provide a good representation of the experimental tests, and reach similar maximum shear forces. The Engineering Masonry model appears to approximate the ascending branch better than the Rankine-Hill model.

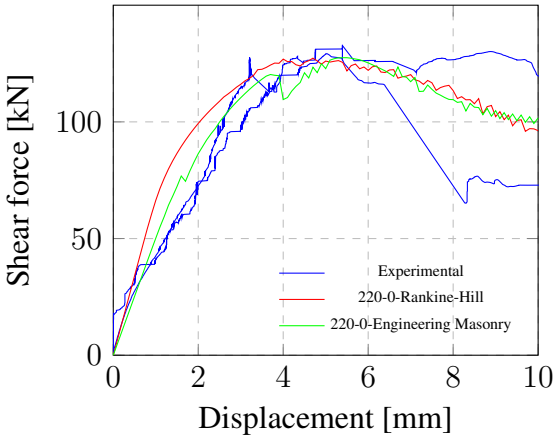

Figure 7: Shear force of masonry wall without SHCC

A 15 mm SHCC overlay was selected since a 10 mm overlay resulted in premature failure and a 20 mm overlay results in a brittle failure with delamination, as found by De Beer [2]. A 15 mm SHCC overlay was applied to the walls and tested. The shear forces obtained for three experimental tests, as well as the Rankine-Hill numerical model are shown in Figure 8. The shear force for the two bare wall specimens are also included in the figure to illustrate the increase in shear resistance that the SHCC provides. The SHCC overlay significantly increases the shear resistance of the masonry wall but the ductility has not been improved. De Jager [4] proposed debonding strips as a means to improve the ductility of the masonry walls.

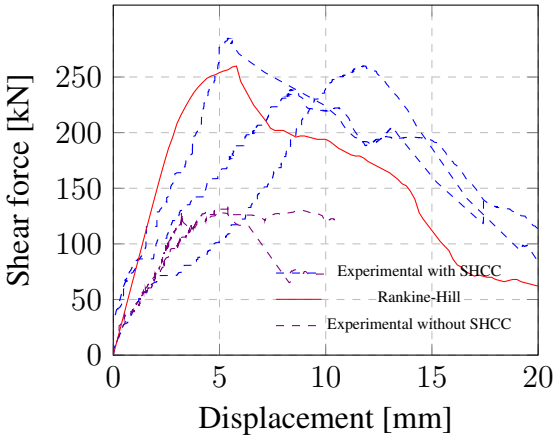

Figure 8: Shear force of masonry wall with SHCC

5 DEBONDING STRIPS

The aim of the debonding strips is to prevent reflective cracking from the masonry wall to the SHCC overlay, cracking in the masonry that reflects straight through to the SHCC overlay. As stress is transferred from the masonry wall to the SHCC overlay through the bonded areas, multiple cracks form in the debonded areas and the stress is distributed more evenly over the SHCC overlay [8]. Figure 9 illustrates the debonding strips applied to the wall before the SHCC overlay is applied. Two diffrent layouts of debonding strips were applied to the masonry wall, (i) 75 mm width strips with a spacing of 150 mm, and (ii) 100 mm width strips with a spacing of 200 mm. Five walls were tested, one representative bare wall and two walls of each layout of debonding strips.

Figure 9: Debonding strips on full scale tests [4]

The shear force against displacement for the walls with debonding strips are illustrated in Figure 10, along with a representative bare wall and the numerical results. It can be seen that the debonding strips can potentially improve the ductility of the masonry walls significantly. The ductility factor of these walls is 2.4 on average with a 0.15 CoV. It should be noted that one of the four tests with strips failed prematurely due to delamination in the bottom right-hand corner of the wall. The delamination occurred due to excessive compression in the SHCC overlay. This was prevented in the final test reported in Table 4 by cutting a 25 mm gap in the SHCC

overlay at the top and bottom of the wall to prevent the concrete beam from inducing additional compressive forces in the SHCC overlay.

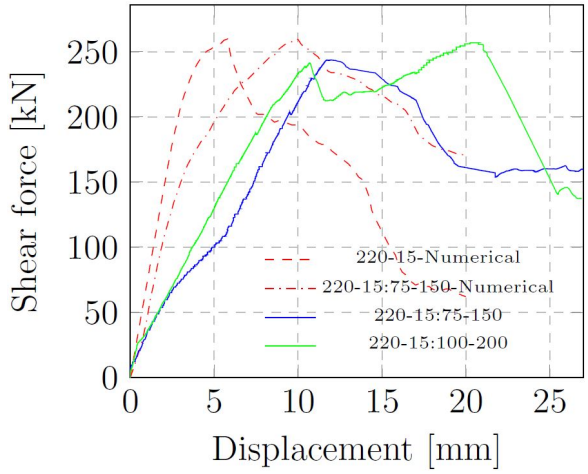

Figure 10: Shear force of masonry with SHCC overlay and debonding strips

The ductility factors for the numerical and experimental specimens are reported in Table 4. The labeling of the specimens is according to the masonry wall thickness, SHCC overlay thickness, debonding strip width, debonding strip spacing, and in the case of multiple tests of the same specimen, the number of the test.

Table 4: Ductility Factors

Specimen	δ_y (mm)	δ_u (mm)	μ	F_p (kN)
N. - Numerical				
220-0	2.6	9.1	3.5	131.3
220-15	2.9	7.3	2.6	259.9
220-15:75-150	4.4	16.8	3.6	260.0
E. - Experimental				
220-0	3.1	6.8	2.2	129.2
220-15	8.8	13.2	1.5	241.7
220-15:75-150:1	6.8	16.8	2.5	218.9
220-15:75-150:2	8.8	17.6	2.0	243.8
220-15:100-200	8.8	23.5	2.7	257.0

The energy contribution factors for the specimens are presented in Table 5 for the given forces F_i (kN). ECF is an expression of energy and consists of the contributions of cracks in the masonry and SHCC overlay, as well as shear slip in the interface between the masonry and the SHCC.

Table 5: ECF values at different forces

F_i	75-150 (avg.)		100-200
	N.	E.	E.
175	1.54	1.31	2.28
200	2.35	1.32	3.10
225	2.31	1.94	3.36

6 CONCLUSION

Computational models to analyse ULM walls with SHCC overlay have been developed and verified by laboratory experiments. Fully bonded SHCC improve the shear resistance of the masonry walls and debonding strips improved the ductility of the masonry walls, by preventing reflective cracking and improving the stress distribution throughout the SHCC overlay. The following conclusions are drawn:

- The in-plane shearing resistance of 220 mm ULM walls are increased by an average of 100% by the application of a 15 mm SHCC overlay.
- The ductility of a masonry wall is not significantly increased by the fully bonded SHCC overlay.
- Diagonal debonding strips can significantly increase the ductility of the retrofitted masonry wall, provided that delamination can be prevented, without compromising the shear resistance gained by the SHCC overlay.

In addition to the modelling of an entire building retrofitted with SHCC, different debonding configurations will be investigated, comprising of but not limited to (a) strips in both directions, (b) horizontal strips, (c) vertical strips, (d) debonding surface in the middle of the wall and (e) different strip widths and spacing.

REFERENCES

[1] SABS 0160. *The structural use of masonry, part 1: Unreinforced masonry walling*. South African Bureau of Standards, South Arica, 1989.

[2] Leon Rhoode De Beer. Developing and testing a sprayable overlay of Strain Hardening Cement-based Composite for retrofitting of unreinforced load bearing masonry walls. (October), 2016.

[3] Hamid Mahmood and Jason M. Ingham. Diagonal Compression Testing of FRP-Retrofitted Unreinforced Clay Brick Masonry Wallettes. *Journal of Composites for Construction*, 15(5):810–820, 2011.

[4] Dirk Jacobus Adriaan de Jager. Assessment of SHCC overlay retrofitting of unreinforced load bearing masonry for seismic resistance. (August), 2018.

[5] DIANA FEA BV. DIANA Theory manual. (March), 2006.

[6] DIANA FEA BV. User ' s Manual Element Library.

[7] G. P. A. G. van Zijl, R de Borst, and JG Rots. A numerical model for the timedependent cracking of cementitious materials. *International Journal for Numerical Methods in Engineering*, 52(7):637–654, 2001.

[8] Yum Mook Lim and Victor C. Li. Durable repair of aged infrastructures using trapping mechanism of engineered cementitious composites. *Cement and Concrete Composites*, 19(4):373–385, 1997.